THE JOURNAL OF PHYSICAL CHEMISTRY A

Article

pubs.acs.org/JPCA

Unanticipated Stickiness of α-Pinene

Published as part of The Journal of Physical Chemistry virtual special issue "Veronica Vaida Festschrift".

Hilary M. Chase,[†,∥] Junming Ho,[‡,∥] Mary Alice Upshur,[†] Regan J. Thomson,[†] Victor S. Batista,[§] and Franz M. Geiger*[,†]

[†]Department of Chemistry, Northwestern University, Evanston, Illinois 60208, United States

[‡]Agency for Science, Technology and Research, Institute of High Performance Computing, 1 Fusionopolis Way #16-16 Connexis North, Singapore 138632

[§]Department of Chemistry, Yale University, P.O. Box 208107, New Haven, Connecticut 06520, United States

Supporting Information

ABSTRACT: The adsorption of α-pinene to solid surfaces is an important primary step during the chemical conversion of this common terpene over mesoporous materials, as well as during the formation of atmospheric aerosols. We provide evidence of tight and loose physisorbed states of α-pinene bound on amorphous SiO_2 as determined by their adsorption entropy, enthalpy, and binding free energies characterized by computational modeling and vibrational sum frequency generation (SFG) spectroscopy. We find that adsorption is partially (40−60%) irreversible over days at 294−342 K and 1 ATM total pressure of helium, which is supported by molecular dynamics (MD) simulations. The distribution of α-pinene orientation remains invariant with temperature and partial pressure of α-pinene. Using the Redlich−Peterson adsorption model in conjunction with a van't Hoff analysis of adsorption isotherms recorded for up to 2.6 Torr α-pinene in 1 ATM total pressure of helium, we obtain ΔS°_{ads}, ΔH°_{ads}, and ΔG°_{ads} values of −57 (±7) J mol^{-1} K^{-1}, −39 (±2) kJ mol^{-1}, and −22 (±5) kJ mol^{-1}, respectively, associated with the reversibly bound population of α-pinene. These values are in good agreement with density functional theory (DFT)-corrected force field calculations based on configurational sampling from MD simulations. Our findings are expected to have direct implications on the conversion of terpenes by silica-based catalysts and for the synthesis of secondary organic aerosol (SOA) in atmospheric chambers and flow tubes.

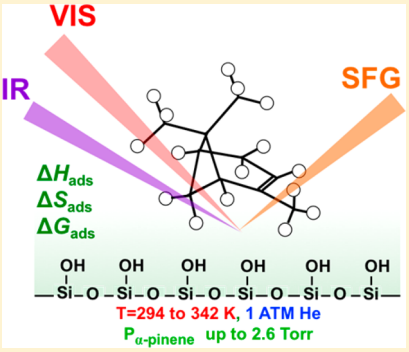

I. INTRODUCTION

Molecular dynamics (MD) simulations have suggested that α-pinene adsorbed to fused silica is rotationally fluid, with two predominant states characterized by significantly different rotational reorientation periods, the population of α-pinene molecules with shorter time scales being stabilized by rotational entropy.[1] This insight into the adsorption mechanism may impact α-pinene conversion into organic frameworks,[2−5] mesoporous materials,[2,3,6−11] and aerosol particle formation,[12−15] particularly due to the highly dynamic variability with which the C═C system may become accessible to oxidation when located in interfacial environments. While MD simulations established a precedent to study heterogeneous interactions of terpenes on solid substrates, the reversibility and thermodynamics of α-pinene interactions with solid substrates have heretofore not been probed nor quantified. Here, we bridge this knowledge gap by pairing vibrational sum frequency generation (SFG) spectroscopy with classical MD simulations to characterize tightly and loosely bound adsorption states of α-pinene on fused silica housed in a temperature-controlled α-pinene vapor/He flow cell. We quantify the extent of reversibility in the adsorption process and determine the thermodynamic parameters of adsorption as well as the distributions of surface-bound molecular orientations.

II. METHODS

IIA. SFG Spectroscopy. A detailed description of the broad-band SFG setup tuned to the C−H stretching region (2800−3200 cm^{-1}) used in this study has been provided in previous work.[16−20] All "room temperature" SFG experiments were performed in a sample cell housed in a laboratory maintained at 21−23 °C temperature and 20−30% relative humidity. We utilized *ssp* and *ppp* polarization combinations, which are used to assess molecular orientation distributions.[21−25]

The flow system and sample cell used in this study are shown in Figure 1. For the temperature-dependent measurements, the design was adapted from our previously published work.[19] Briefly, a home-built aluminum flow cell (Figure 1A) of similar volume (roughly 7 cm^3) to our previously described Teflon cell was outfitted with two low density cartridge heaters (Omega Engineering, LDC00014) connected to a Eurotherm power

Received: December 16, 2016
Published: January 19, 2017

DOI: 10.1021/acs.jpca.6b12653
J. Phys. Chem. A 2017, 121, 3239−3246

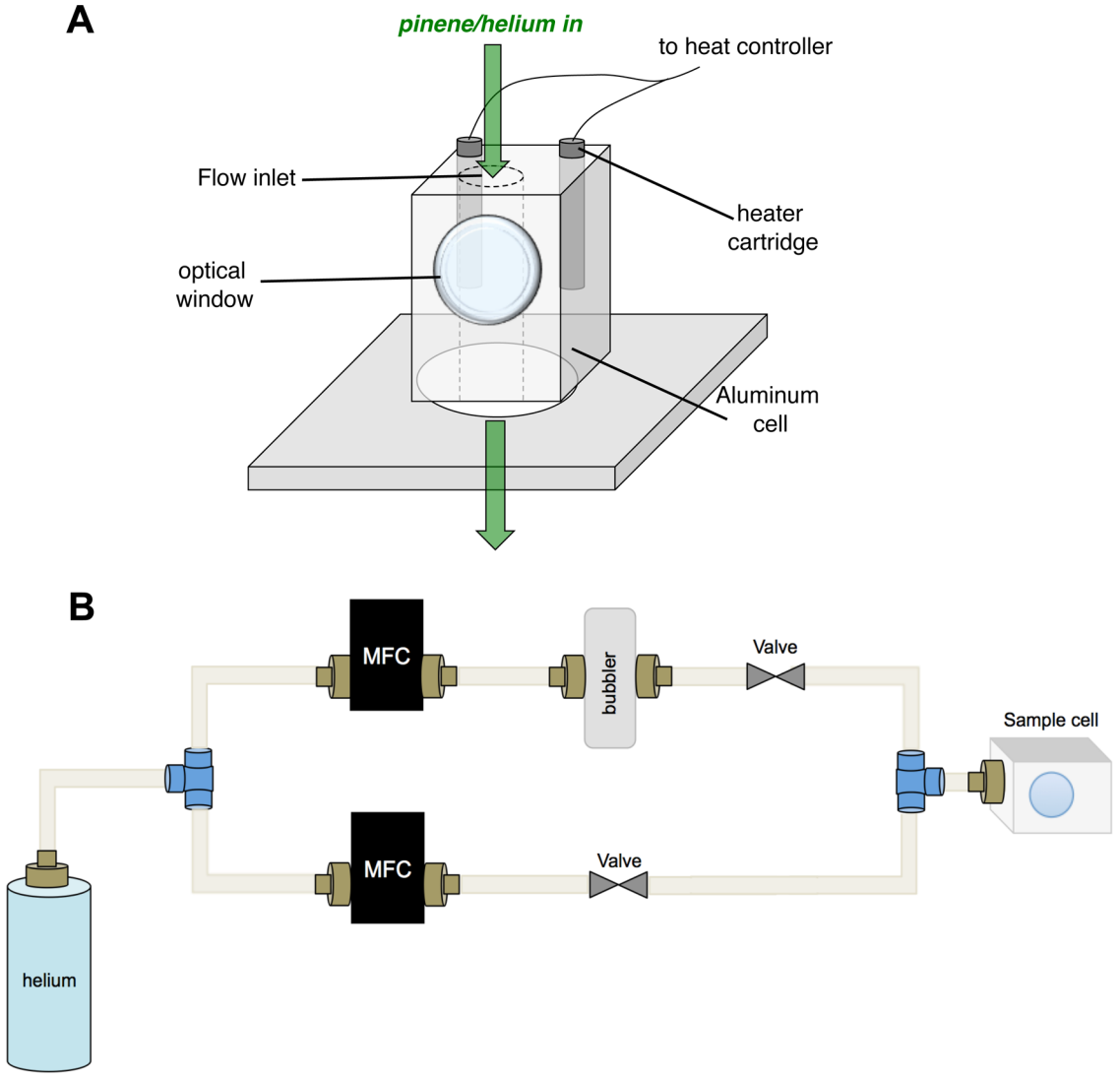

Figure 1. Aluminum sample temperature cell used in the temperature-dependent SFG experiments described in the Methods section (A). This sample cell is hooked up to the α-pinene/He flow setup shown in (B).

supply/temperature controller, and thermal feedback was provided with a Type K thermocouple (McMaster Carr). Before each experiment, the flow cell, the Viton O-ring, and the optical window were rinsed with HPLC-grade methanol (when using just the Teflon flow cell described in ref 10) and Millipore water (when using both the Teflon and the aluminum flow cells), and then dried with nitrogen gas and subsequently in an oven, as described earlier.[19] The Viton O-ring, Teflon cell, and windows were plasma-cleaned for ~10−12 min immediately before acquiring SFG spectra. In the spectroscopy experiments, an IR-grade fused silica window was pressed against a Viton O-ring sealing it to the flow cell. The flow setup (Figure 1B) consisted of a dry helium flow line, connected by corrugated tubing (corrugated FEP tubing, Cole-Parmer), and an α-pinene vapor flow line, wherein dry helium was passed through a bubbler containing roughly 10 mL of liquid (−)-α-pinene (98% purity, Sigma-Aldrich). Electronic mass flow controllers (MFCs) (Alicat Scientific) were used to regulate flow rates for both lines. Flow rates are reported in SLPM (standard liter per minute).

For the α-pinene adsorption isotherm measurements, we employed a total flow rate of either 5 or 10 SLPM by adjusting the relative flow rates of dry helium and helium flowing through the α-pinene bubbler. The SFG spectra were collected within ca. 20 s after adjusting the gas flow on the MFCs. The room temperature adsorption isotherm reported is an average of eight individual isotherms, whereas the higher temperature isotherms are an average of duplicates or triplicates.

Fourier Transform Infrared (FTIR) spectroscopy was used for experimental controls (showing, most importantly, no residual α-pinene in the flow lines or the flow cell when flowing helium following α-pinene flow, at least within the FTIR sensitivity) and α-pinene vapor pressure calibration. These experiments are detailed in SI Section 3.

IIB. Computational Methods. MD simulations have been performed as described thoroughly in a recent study.[1] Briefly, MD simulations were performed on a model of amorphous silica based on a 11.5 × 11.5 × 2 nm slab adopted from the work of Cruz-Chu et al.,[26] with a surface concentration of [α-pinene] = 1/nm^2 (i.e., 130 α-pinene molecules). We employed CHARMM force field parameters for amorphous silica, optimized to reproduce the water contact angle (denoted by CWCA FF), and CHARMM General force field (CGenFF)

DOI: 10.1021/acs.jpca.6b12653
J. Phys. Chem. A 2017, 121, 3239−3246

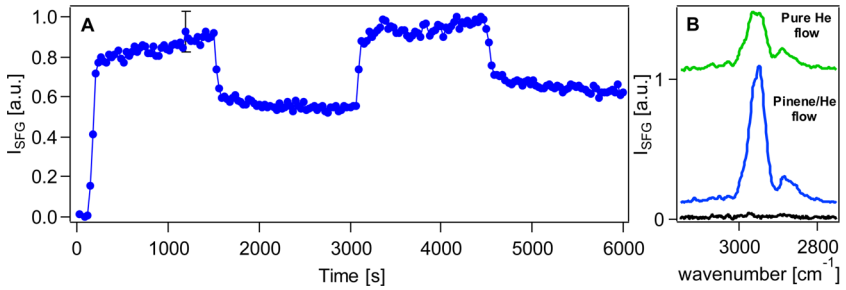

Figure 2. Average on−off trace for 5 SLPM α-pinene and He normalized to the maximum *ssp*-polarized SFG signal intensity (A), and the individual *ssp*-polarized SFG spectra (B) of pure He flow (black trace), 5 SLPM α-pinene flow (blue trace, offset), and 5 SLPM He flow after α-pinene exposure (green trace, offset).

parameters for α-pinene.[26] All MD simulations were carried out using the NAMD program.[27]

The enthalpy of adsorption (at 298 K) was estimated for individual α-pinene molecules by randomly selecting 400 frames along a given 10 ns trajectory. The binding energy was calculated for each frame and the enthalpy of adsorption was obtained as the average over all frames. The uncertainty in the point estimate of the enthalpy of adsorption corresponds to two standard deviations (2σ) based on five independent simulations. The adsorption free energy was estimated considering that a third of the translational entropy is lost upon adsorption,[28,29] with α-pinene adsorbed on the silica surface as shown by MD simulations. Based on the ideal gas translational partition function, the resulting estimate corresponds to a ΔS_{ads} of approximately −57 J mol^{-1} K^{-1}. The contact area between each α-pinene molecule and the silica surface was obtained from the difference between the surface area of the separate fragments, and the corresponding adsorbed configuration. A scaling factor of 1.2 was applied to the van der Waals radii (defined in VMD), and reported contact areas correspond to the averages over all 400 frames.

The analysis of the electronic contributions to the interactions between α-pinene and the silica surface involved density functional theory (DFT, ωB97XD/6-31G(d)) calculations[30] on a cluster model. A bowl-shaped cluster (304 atoms) was carved from the silica slab used for the MD simulations, and the dangling bonds were capped with hydrogen atoms. Snapshots of α-pinene molecule at different orientations above the cluster were selected from the MD trajectory and the DFT interaction energies were evaluated by carrying out single-point calculations including counterpoise correction for basis set superposition error.[31,32] The analysis indicated that the CHARMM force field overestimates on average the binding interaction by ca. 12 kJ mol^{-1} relative to ωB97XD/6-31G(d) values. Therefore, we applied this correction factor to the CHARMM adsorption enthalpies as described in the Supporting Information (Section S8).

III. RESULTS AND DISCUSSION

IIIA. SFG Experiments of α-Pinene Adsorption to Silica Indicate Partial Reversibility over a Long Time Scale, Revealing Two Bound States of α-Pinene. We observe partial reversibility of α-pinene adsorption to silica (Figure 2) by alternating between α-pinene vapor/He flow and pure He flow at room temperature. We consistently observe a ∼ 30−60% decrease in the *ssp*-polarized SFG signal intensity when flowing He gas across the optical windows after 2.3, 0.1, and 0.02 Torr α-pinene exposures (see Supporting Information, Section S7). Considerable SFG signal intensity was detected for up to 3 days after an initial α-pinene exposure lasting less than 10 min and subsequently leaving the optical window out under ambient conditions (albeit covered in a Petri dish). Further, we observe persistent SFG signal, albeit often decreased signal intensities, after flowing He or N_2 at flow rates of up to 10 SLPM. We observe nearly complete loss in signal intensity following α-pinene exposure when we rinse the optical window with HPLC-grade methanol and allow the methanol to evaporate. We carried out analogous on−off experiments at 69 °C, where α-pinene has a higher vapor pressure of ∼45 Torr, and observed similar adsorption reversibility to that at room temperature, which suggests that the extent of reversibility may be independent of vapor pressure.

To further understand these results, we found that the extent of adsorption reversibility of α-pinene to fused silica between room temperature and 69 °C differs from that observed for hexane, which has a higher vapor pressure (∼120 Torr at room temperature), adsorbed to fused silica. We recorded, in triplicate, hexane vapor/SiO_2 on−off traces and observed that the adsorption process is fully reversible over the time scale of our measurements. In fact, within 1 min, the SFG signal was reduced to nearly the baseline. The average hexane on−off trace is given in the Supporting Information (Section S4). While hexane and α-pinene are hydrocarbons with very different molecular structures, this finding further suggests that vapor pressure alone may not determine the reversibility extent. The difference in these adsorption behavior may be due to the fact that the crater-like pockets on the silica surface may better accommodate the bicyclic structure of α-pinene than the linear hexane molecule. Future work will be carried out to further connect the structure of a number of hydrocarbons to adsorption reversibility.

We also recorded an on−off trace for α-pinene using a CaF_2 substrate and observed partial reversibility, just like with fused silica. This result suggests that the binding of α-pinene to fused silica is not uniquely dominated or necessarily enhanced by interactions with the Si−OH groups on the substrate surface.

IIIB. DFT-Corrected CHARMM Force-Field Calculations of ΔG_{ads}, ΔH_{ads}, and ΔS_{ads}. The consistent observation of partial reversibility of α-pinene bound to fused silica at room temperature suggests that there may be two types of α-pinene on the silica substrate: a "loosely bound" state of α-pinene that desorbs readily upon helium flow, and a "tightly bound" population. These findings support our recent work,[1] where we employed classical MD simulations to sample 130 α-pinene molecules on a fused silica slab. We identified a population (ca. 50% of the total population) of α-pinene molecules stabilized by rotational entropy, with a calculated rotational entropic

DOI: 10.1021/acs.jpca.6b12653
J. Phys. Chem. A 2017, 121, 3239−3246

stabilization energy relative to the static state of ∼11 kJ mol^{-1} at 300 K. We determined that the other half of the α-pinene population has a rotational reorientation period of ∼2500 ps, significantly longer than the 50 ps rotational reorientation time of the rotationally fluid state. Long rotational reorientation times suggest that α-pinene molecules are rotationally hindered, exhibiting less rotational entropic stabilization, and are more tightly bound to the silica surface.

To further investigate the nature of the binding modes, we obtained thermodynamic parameters for the adsorption and desorption process by computational modeling. The interaction energy with the silica surface was averaged over 400 snapshots sampled along a 10 ns MD trajectory to yield the adsorption enthalpy for individual α-pinene molecules. Figure 3 shows the

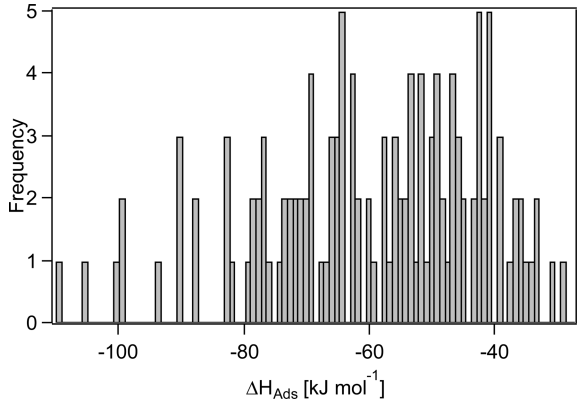

Figure 3. Histogram showing the distribution of ΔH°_{ads} values calculated from MD simulations.

distribution of the DFT-corrected adsorption enthalpies, which span over the range from −37 to −125 kJ mol^{-1}. The distribution of adsorption enthalpies reflects the heterogeneity of the amorphous silica surface. Figure 4A shows a snapshot from the MD simulations of selected α-pinene molecules with very different adsorption enthalpies. The surface is undulating, and is covered with "craters" of different shapes and sizes, some of which can accommodate α-pinene molecules better than others. The molecule with the strongest adsorption enthalpy is shown to fit snugly in one of the craters on the surface. As hypothesized in our earlier work,[1] tightly bound α-pinene molecules, with long rotational reorientation times through hindered rotations on the surface, are associated with larger van der Waals contact with the surface. This is confirmed in Figure 4B where there is a strong and direct correlation between the adsorption enthalpy and surface contact area.

Since adsorption/desorption of α-pinene on silica is approximately barrierless, we estimated the barrier to desorption to be that of the adsorption free energy, i.e., $\Delta G_{ads} \sim \Delta G^{\ddagger}$. Accordingly, the desorption rate constant for each α-pinene molecule on the model surface was computed using enthalpy of adsorption obtained from MD simulations, and a uniform $\Delta S_{ads} = -57$ J mol^{-1} K^{-1} estimated from the loss of a third of translational entropy.[28,29] The rate constants were then averaged over all molecules (N = 130) as follows:

$$\langle k \rangle = \frac{1}{N}\frac{k_B T}{h}\sum_{i=1}^{N}\exp(-\Delta G_i/RT) \quad (1)$$

According to the ensemble average of eq 1, the "loosely" bound α-pinene molecules (i.e., those associated with reversible

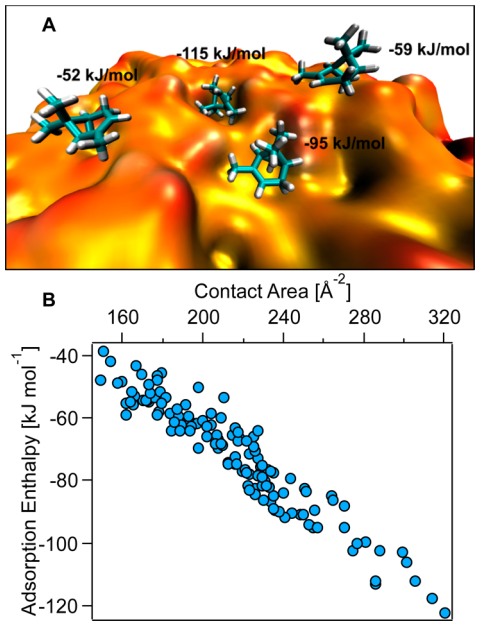

Figure 4. (A) MD snapshot of selected α-pinene on part of the fused silica slab. Calculated adsorption enthalpy (in kJ/mol) are also shown. (B) The XY plot of adsorption enthalpy versus surface contact area for 130 α-pinene molecules.

adsorption) define the population that contributes most to the desorption process. From five trajectories, we obtained average rate constants $\langle k \rangle$ in eq 1 that yielded $\Delta G_{ads} = -20 \pm 4$ kJ mol^{-1} and $\Delta H_{ads} = -37 \pm 4$ kJ mol^{-1} (with $\Delta S_{ads} = -57$ J mol^{-1} K^{-1}). As discussed next, the calculated values are in good agreement with the results obtained from our experimental adsorption isotherms.

IIIC. Experimental Adsorption Isotherms Are in Close Agreement with Values Computed from MD Simulations. The adsorption isotherms were obtained by integrating the *ssp*-polarized SFG signal intensity over the 2800−3050 cm^{-1} range for each spectrum, and then plotting the square root of this integral[33,34] as a function of α-pinene partial pressure. We obtained adsorption isotherms at five different temperatures (Figure 5A). We fit each isotherm to obtain temperature-dependent K°_{ads} values after correcting for the standard state atmospheric pressure (760 Torr).[29] Ln(K°_{ads}) vs.

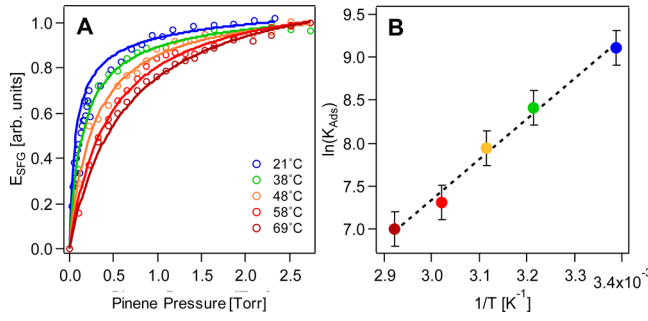

Figure 5. Square root of the *ssp*-polarized SFG signal intensity (SFG E-field) as a function of α-pinene pressure were plotted at varying temperatures (A), and were normalized to the max E-field per temperature. The adsorption isotherms were fit to the Redlich−Peterson adsorption model, and subsequent K_{ads} values were used to construct a van't Hoff plot (B) to determine ΔG°_{ads}, ΔH°_{ads}, and ΔS°_{ads}.

DOI: 10.1021/acs.jpca.6b12653
J. Phys. Chem. A 2017, 121, 3239−3246

T was plotted and fit to the the van't Hoff linear equation (Figure 5B), and ΔH°_{ads} and ΔS°_{ads} values were obtained by the slope and y-intercept, respectively. The uncertainties in these values are determined by the standard deviation of the fit values (Figure 5B). Specifically, we carried out a global fit analysis for all adsorption isotherms using various adsorption models, including Langmuir, Langmuir−Freundlich, and the dual-site variants of these models (detailed in Section S5 in the SI). We have also considered the Redlich−Peterson (R−P) adsorption model, a "useful adsorption isotherm"[35] that is a hybrid of the Langmuir and Freundlich isotherm models applicable for both heterogeneous and homogeneous surfaces.[36−38] The expressions for the Langmuir and Redlich−Peterson models are shown in eq 2 and 3, respectively:

$$f(P) = \frac{a \times KP}{1 + KP} \tag{2}$$

$$f(P) = \frac{AP}{1 + BP^{g}} \tag{3}$$

where a and K in eq 2 are the monolayer coverage scaling factor and adsorption constant (in units of $Torr^{-1}$), and A and B from eq 3 are the R−P isotherm constants, P is the partial pressure of α-pinene in Torr, and g is a unitless parameter indicative of the extent of heterogeneity in the bound layer. When $g \neq 1$, the system is heterogeneous and thus deviates from the Langmuir model, and when $g = 1$, expression 3 reduces to the Langmuir model. We ultimately obtain the equilibrium constant for adsorption (K°) after applying standard state corrections (Section S5 in the SI).

Table 1 shows the thermodynamic parameters from various adsorption model fits derived from the familiar van't Hoff expression. With the exception of the dual-site-irreversible model, all models yield comparable Gibbs free energies of adsorption around 22 kJ mol^{-1}. On the other hand, enthalpies ranged between 23 to 48 kJ mol^{-1}, while entropies ranged from 7 to 83 J mol^{-1} K^{-1}. The Redlich−Peterson model yields a ΔH°_{ads} of −39 ± 2 kJ mol^{-1}, a ΔS°_{ads} of −57 ± 7 J $mol^{-1}K^{-1}$, and a ΔG°_{ads} of −22 ± 5 kJ mol^{-1}. The Langmuir adsorption model also provided a similar value of ΔG°_{ads} (−22 ± 7 kJ mol^{-1}), although ΔH°_{ads} (−30 ± 3 kJ mol^{-1}) and ΔS°_{ads} (−28 ± 9 J $mol^{-1}K^{-1}$) differed significantly from the values obtained with the Redlich-Peterson model. This difference is curious since the Redlich−Peterson and the Langmuir models converge as g in eq 3 approaches unity. The fitted g-values obtained from the R−P model ranged from 0.95 ± 0.01 (at 21 °C) to 0.99 ± 0.04 (at 68 °C) suggesting that ΔG°_{ads} should be very similar in both models. This is indeed the case (as shown in Tables S3 and S4), where the Gibbs free energies of adsorption from the two models differ by less than 1 kJ mol^{-1} across various temperatures. The differences in the resulting ΔH°_{ads} and ΔS°_{ads} from the Redlich−Peterson and Langmuir models, therefore, reflect the sensitivity of these values to minute changes in ΔG°_{ads} used in the van't Hoff equation.

Overall, we consider the Redlich−Peterson model to be the most reliable for the following reasons: (1) There is overall good agreement between R−P and theoretical thermodynamic parameters. The experimental and theoretical ΔH_{ads} are in close agreement. This is also the case for the values of ΔS_{ads} and ΔG_{ads}; however, comparison between theory and experiment for these quantities is complicated by definitions of standard states. (2) The value for ΔS°_{ads} is physically reasonable. The other models (Langmuir, Langmuir−Freundlich, Dual-Site Langmuir−Freundlich) either display ΔS°_{ads} that are less than a sixth of the translational entropy, or ΔH_{ads} values that differ significantly from simulations.

Table 1. Thermodynamic Parameters from Various Adsorption Model Fits

model	$-\Delta H^{\circ}_{ads}$ (kJ mol^{-1})	$-\Delta S^{\circ}_{ads}$ (J mol^{-1} K^{-1})	$-\Delta G^{\circ}_{ads}$ (kJ mol^{-1})
Langmuir	**30 ± 3**	**28 ± 9**	**22 ± 7**
dual-site Langmuir	48 ± 7	83 ± 24	23 ± 5
Langmuir−Freundlich	25 ± 5	12 ± 16	21 ± 7
dual-site Langmuir Freundlich	23 ± 4	7 ± 12	21 ± 4
dual site with irreversibility	27 ± 3	74 ± 9	5 ± 4
Redlich−Peterson	**39 ± 2**	**57 ± 7**	**22 ± 5**
MD-based values	**37 ± 4**	**57**[a]	**20 ± 4**[a]

[a]Comparison of experimental and theoretical entropies (and consequently Gibbs free energy) of adsorption is complicated by standard state issues. The former defines a reference state for 1 atm in the gas phase and half-coverage of surface sites, while the theoretical value is estimated from the loss of one translational degree of an ideal gas at 1 atm.

IIID. Experiments and Simulations Reveal Negligible Changes in Molecular Orientation but Considerable Decreases in Surface Coverage with Increasing Temperature. Changes in molecular orientation distributions with increasing temperature and/or partial pressure could contribute to changes in SFG intensity. This can be determined by measuring SFG spectra in both *ssp* and *ppp* polarization combinations. Specifically, by evaluating the *ppp*/*ssp* ratio of the SFG amplitudes of a particular oscillator, the molecular orientation can usually be deduced using well-established SFG selection rules.[25,39−45] We did not carry out quantitative orientation analyses since the individual peaks in the SFG spectrum of α-pinene are difficult to assign, although reliable spectral assignments are now just beginning to emerge.[46] Rather, given the negligible variations in line shape with applied α-pinene partial pressure, we compare the ratios of the *ppp*- and *ssp*-polarized SFG intensities integrated from 2800 to 3050 cm^{-1} as a function of α-pinene vapor pressure (Supporting Figure S1). An average of two trials indicates that there are negligible changes in the average molecular orientation of α-pinene, upon increasing surface coverage or α-pinene partial pressure. This result indicates that our measured SFG spectra, forming the basis for our adsorption isotherm analysis, are not influenced by changes in molecular orientation induced by changes in the α-pinene partial pressure. Furthermore, this result further suggests that no multilayers are forming. Mass measurements by quartz crystal microbalance, which are currently unavailable, will be needed to provide further details regarding the absolute amount of adsorbed pinene.

Figure 6A shows a decrease in the SFG *ssp*-polarized signal intensity with increasing temperature. This finding suggests that (a) there is a change in the distribution of molecular orientations of α-pinene upon increasing temperatures and/or (b) fewer α-pinene molecules are bound to the fused silica surface. Therefore, we plotted the *ppp*/*ssp* area ratios of the SFG signals as a function of temperature, along with the percent reversibility obtained from duplicates for the lowest and highest surveyed temperature (Figure 6B). We find that there are negligible changes in *ppp*/*ssp* area ratios, suggesting that

DOI: 10.1021/acs.jpca.6b12653
J. Phys. Chem. A 2017, 121, 3239−3246

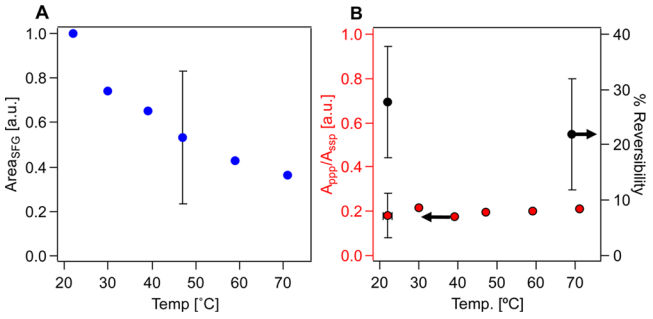

Figure 6. Plot of *ssp*-polarized SFG signal area ($Area_{SFG}$) as a function of temperature (A). Two trials have been averaged, and all areas have been corrected for incident visible and IR powers. (B) Extent of reversibility at two different temperatures (black markers) and A_{PPP}/A_{SSP} ratios as a function of temperature (red markers). Error bars indicate standard deviations of averaging trials.

there are negligible changes in molecular orientation as a function of temperature. Supporting this finding are MD simulations that track the trajectories of 130 α-pinene molecules at 340 K over 10 ns, resulting in negligible changes in the molecular orientation distribution. The distributions of molecular orientations over the two trajectories at 300 and 340 K are given in the Supporting Information (Section S6).

Given the negligible changes in molecular orientations with increasing temperature, we attribute the observed decreases in SFG signal intensity with increasing temperature to desorption of α-pinene molecules from the silica surface. From the MD trajectory of α-pinene adsorbed to silica at 340 K, as described in the previous section, we extracted two new rotational reorientation times by fitting the rotational reorientation autocorrelation function of the 10 ns trajectory to a double exponential fit function, as reported recently.[1] From the fit (Section S6 in the Supporting Information), we extract a τ_1 value of 1980 ± 40 ps and a τ_2 value of 23 ± 0.5 ps at 340 K, whereas at 300 K these values were 2500 and 50 ps, respectively. The results suggest that the α-pinene population that is tightly bound at room temperature is more loosely bound at 340 K. Since we have ruled out large changes in molecular orientation in the previous section, less α-pinene molecules are likely to populate the surface at higher temperature.

V. CONCLUSION AND IMPLICATIONS

We have provided experimental and computational evidence of two adsorption states of α-pinene on fused silica. We have shown that the adsorption of α-pinene to fused silica is partially reversible over the time scale of our measurements (days) at room temperature and at elevated temperatures (~40 Torr), whereas hexane (~120 Torr) adsorption to fused silica at room temperature is fully reversible within minutes. This finding suggests that the adsorption reversibility may be independent of vapor pressure, although future work is warranted. MD simulations have shown that the two populations of α-pinene molecules exhibit vastly different temperature-dependent rotational reorientation times. A loosely bound population of molecules having short rotational reorientation lifetimes, that desorb readily as detected by SFG, are likely stabilized by rotational entropy and have less van der Waals contact with the substrate. Furthermore, partial reversibility of adsorption to CaF_2 suggests that irreversible adsorption is not uniquely connected to interactions with Si−OH groups on the silica surface, but that it may indeed be substrate-general. Additionally, we have fully quantified the thermodynamics of adsorption of the ensemble of α-pinene molecules by temperature-dependent SFG measurements and MD simulations, showing that binding is heterogeneous, as reflected in our van't Hoff analysis of the Redlich−Peterson adsorption model fitted to the experimental data, as well as the thermodynamic calculations obtained from the simulations. Specifically, for up to 2.6 Torr α-pinene in 1 ATM total pressure of helium, we obtain ΔS°_{ads}, ΔH°_{ads}, and ΔG°_{ads} values of −57 (±7) J mol^{-1}K^{-1}, −39 (±2) kJ mol^{-1}, and −22 (±5) kJ mol^{-1}, respectively, from experiments. DFT-corrected MD results show that ΔH_{ads} of −37 ± 4 kJ mol^{-1} at 298 K that is in closest agreement with the Redlich−Peterson adsorption model. Other common adsorption models do not provide satisfactory agreement between theory and experiments.

Finally, we have shown by MD simulations and SFG spectroscopy that the ensemble average molecular orientation of α-pinene does not change as a function of temperature and vapor pressure, and that the α-pinene surface coverage decreases with increasing temperatures for the conditions probed by our experiments. The possible implication of our results for chemical conversion of terpenes like α-pinene over silica-based catalyst surfaces is that these sustainable feedstocks for polymer synthesis[47] are likely to exhibit unexpected long surface lifetimes, which should aid in catalytic transformations. The implication of our results for preparing and analyzing laboratory models of secondary organic aerosol (SOA) from α-pinene ozonolysis is that the internal surfaces of the materials used to construct the environmental chambers or flow tubes for SOA preparation are likely to be covered, for extended times (i.e., lasting for days), with α-pinene, whose further reactivity may influence chamber studies in ways that may now be quantifiable better than before. Future work will address the adsorption dynamics of other naturally abundant terpene compounds.

■ ASSOCIATED CONTENT

Supporting Information

The Supporting Information is available free of charge on the ACS Publications website at DOI: 10.1021/acs.jpca.6b12653.

(PDF)

■ AUTHOR INFORMATION

ORCID

Junming Ho: 0000-0001-9381-924X
Regan J. Thomson: 0000-0001-5546-4038
Victor S. Batista: 0000-0002-3262-1237
Franz M. Geiger: 0000-0001-8569-4045

Author Contributions

‖These authors contributed equally to this work.

Notes

The authors declare no competing financial interest.

■ ACKNOWLEDGMENTS

H.M.C. gratefully acknowledges Alicia McGeachy for valuable discussions regarding adsorption models, as well as support from a National Science Foundation (NSF) Graduate Research Fellowship under Grant No. DGE-1324585 and the Institute for Sustainability and Energy at Northwestern (ISEN). J.H. gratefully acknowledges support from the Agency for Science,

DOI: 10.1021/acs.jpca.6b12653
J. Phys. Chem. A 2017, 121, 3239−3246

Technology and Research (Singapore) and the NCI for generous allocation of computer time. M.A.U. gratefully acknowledges support from a National Aeronautics and Space Administration Earth and Space (NASA ESS) Fellowship and an NSF Graduate Research Fellowship and a P.E.O. Scholar Award. F.M.G., R.J.T., and V.S.B. acknowledge support from NSF Grant CHE-1607640, and computer time from EMSL. V.S.B. acknowledges support from NSF Grant CHE-1465108. This work made use of the FTIR spectrometer in the Integrated Molecular Structure Education and Research Center (IMSERC, Northwestern University).

REFERENCES

(1) Ho, J.; Psciuk, B. T.; Chase, H. M.; Rudshteyn, B.; Upshur, M. A.; Fu, L.; Thomson, R. J.; Wang, H.-F.; Geiger, F. M.; Batista, V. S. Sum Frequency Generation Spectroscopy and Molecular Dynamics Simulations Reveal a Rotationally Fluid Adsorption State of α-Pinene on Silica. *J. Phys. Chem. C* **2016**, *120*, 12578−12589.

(2) Cánepa, A. L.; Chanquía, C. M.; Vaschetti, V. M.; Eimer, G. A.; Casuscelli, S. G. Biomass toward Fine Chemical Products: Oxidation of α-Pinene over Sieves Nanostructured Modified with Vanadium. *J. Mol. Catal. A: Chem.* **2015**, *404*−*405*, 65−73.

(3) Hartlieb, K. J.; Holcroft, J. M.; Moghadam, P. Z.; Vermeulen, N. A.; Algaradah, M. M.; Nassar, M. S.; Botros, Y. Y.; Snurr, R. Q.; Stoddart, J. F. Cd-Mof: A Versatile Separation Medium. *J. Am. Chem. Soc.* **2016**, *138*, 2292−2301.

(4) Maksimchuk, N. V.; Kovalenko, K. A.; Arzumanov, S. S.; Chesalov, Y. A.; Melgunov, M. S.; Stepanov, A. G.; Fedin, V. P.; Kholdeeva, O. A. Hybrid Polyoxotungstate/Mil-101 Materials: Synthesis, Characterization, and Catalysis of H2o2-Based Alkene Epoxidation. *Inorg. Chem.* **2010**, *49*, 2920−2930.

(5) Kholdeeva, O. A.; Skobelev, I. Y.; Ivanchikova, I. D.; Kovalenko, K. A.; Fedin, V. P.; Sorokin, A. B. Hydrocarbon Oxidation over Fe- and Cr-Containing Metal-Organic Frameworks Mil-100 and Mil-101-a Comparative Study. *Catal. Today* **2014**, *238*, 54−61.

(6) Ravasio, N.; Zaccheria, F.; Guidotti, M.; Psaro, R. Mono- and Bifunctional Heterogeneous Catalytic Transformation of Terpenes and Terpenoids. *Top. Catal.* **2004**, *27*, 157−168.

(7) Maksimchuk, N. V.; Melgunov, M. S.; Mrowiec-Białoń, J.; Jarzębski, A. B.; Kholdeeva, O. A. H2o2-Based Allylic Oxidation of A-Pinene over Different Single Site Catalysts. *J. Catal.* **2005**, *235*, 175−183.

(8) Roberge, D. M.; Buhl, D.; Niederer, J. P. M.; Hölderich, W. F. Catalytic Aspects in the Transformation of Pinenes to P-Cymene. *Appl. Catal., A* **2001**, *215*, 111−124.

(9) Frattini, L.; Isaacs, M. A.; Parlett, C. M. A.; Wilson, K.; Kyriakou, G.; Lee, A. F. Support Enhanced α-Pinene Isomerization over Hpw/Sba-15. *Appl. Catal., B* **2017**, *200*, 10−18.

(10) Chanquía, C. M.; Canepa, A. L.; Winkler, E. L.; Rodriguez-Castellon, E.; Casuscelli, S. G.; Eimer, G. A. Nature of Active Vanadium Nanospecies in Mcm-41 Type Catalysts for Olefins Oxidation. *Mater. Chem. Phys.* **2016**, *175*, 172−179.

(11) Ajaikumar, S.; Golets, M.; Larsson, W.; Shchukarev, A.; Kordas, K.; Leino, A. R.; Mikkola, J. P. Effective Dispersion of Au and Au-M (M = Co, Ni, Cu and Zn) Bimetallic Nanoparticles over Tio2 Grafted Sba-15: Their Catalytic Activity on Dehydroisomerization of Alpha-Pinene. *Microporous Mesoporous Mater.* **2013**, *173*, 99−111.

(12) Zhang, X.; McVay, R. C.; Huang, D. D.; Dalleska, N. F.; Aumont, B.; Flagan, R. C.; Seinfeld, J. H. Formation and Evolution of Molecular Products in α-Pinene Secondary Organic Aerosol. *Proc. Natl. Acad. Sci. U. S. A.* **2015**, *112*, 14168−14173.

(13) Shrestha, M.; Zhang, Y.; Ebben, C. J.; Martin, S. T.; Geiger, F. M. Vibrational Sum Frequency Generation Spectroscopy of Secondary Organic Material Produced by Condensational Growth from α-Pinene Ozonolysis. *J. Phys. Chem. A* **2013**, *117*, 8427−8436.

(14) Kroll, J. H.; Seinfeld, J. H. Chemistry of Secondary Organic Aerosol: Formation and Evolution of Low-Volatility Organics in the Atmosphere. *Atmos. Environ.* **2008**, *42*, 3593−3624.

(15) Lopez-Hilfiker, F. D.; et al. Phase Partitioning and Volatility of Secondary Organic Aerosol Components Formed from α-Pinene Ozonolysis and Oh Oxidation: The Importance of Accretion Products and Other Low Volatility Compounds. *Atmos. Chem. Phys.* **2015**, *15*, 7765−7776.

(16) Achtyl, J. L.; Buchbinder, A. M.; Geiger, F. M. Hydrocarbon on Carbon: Coherent Vibrational Spectroscopy of Toluene on Graphite. *J. Phys. Chem. Lett.* **2012**, *3*, 280−282.

(17) Chase, H. M.; Psciuk, B. T.; Strick, B. F.; Thomson, R. J.; Batista, V. S.; Geiger, F. M. Beyond Local Group Modes in Sum Frequency Generation Spectroscopy. *J. Phys. Chem. A* **2015**, *119*, 3407−3414.

(18) Ebben, C. J.; Strick, B. F.; Upshur, M. A.; Chase, H. M.; Achtyl, J. L.; Thomson, R. J.; Geiger, F. M. Towards the Identification of Molecular Constituents Associated with the Surfaces of Isoprene-Derived Secondary Organic Aerosol (Soa) Particles. *Atmos. Chem. Phys.* **2014**, *14*, 2303−2314.

(19) Shrestha, M.; Zhang, Y.; Upshur, M. A.; Liu, P.; Blair, S. L.; Wang, H.-f.; Nizkorodov, S. A.; Thomson, R. J.; Martin, S. T.; Geiger, F. M. On Surface Order and Disorder of α-Pinene-Derived Secondary Organic Material. *J. Phys. Chem. A* **2015**, *119*, 4609−4617.

(20) Stokes, G. Y.; Buchbinder, A. M.; Gibbs-Davis, J. M.; Scheidt, K. A.; Geiger, F. M. Heterogenous Ozone Oxidation Reactions of 1-Pentene, Cyclopentene, Cyclohexene, and Menthenol Derivative Studied by Sum Frequency Generation. *J. Phys. Chem. A* **2008**, *112*, 11688−11698.

(21) Baldelli, S.; Bao, J.; Wu, W.; Pei, S.-s. Sum Frequency Generation Study on the Orientation of Room-Temperature Ionic Liquid at the Graphene−Ionic Liquid Interface. *Chem. Phys. Lett.* **2011**, *516*, 171−173.

(22) Zhuang, X.; Miranda, P. B.; Kim, D.; Shen, Y. R. Mapping Molecular Orientation and Conformation at Interfaces by Surface Nonlinear Optics. *Phys. Rev. B: Condens. Matter Mater. Phys.* **1999**, *59*, 12632−12640.

(23) Tyrode, E.; Johnson, C. M.; Baldelli, S.; Leygraf, C.; Rutland, M. W. A Vibrational Sum Frequency Spectroscopy Study of the Liquid−Gas Interface of Acetic Acid−Water Mixtures: 2. Orientation Analysis. *J. Phys. Chem. B* **2005**, *109*, 329−341.

(24) Cecchet, F.; Lis, D.; Guthmuller, J.; Champagne, B.; Caudano, Y.; Silien, C.; Addin Mani, A.; Thiry, P. A.; Peremans, A. Orientational Analysis of Dodecanethiol and P-Nitrothiophenol Sams on Metals with Polarisation-Dependent Sfg Spectroscopy. *ChemPhysChem* **2010**, *11*, 607−615.

(25) Wang, H. F.; Gan, W.; Lu, R.; Rao, Y.; Wu, B. H. Quantitative Spectral and Orientational Analysis in Surface Sum Frequency Generation Vibrational Spectroscopy (Sfg-Vs). *Int. Rev. Phys. Chem.* **2005**, *24*, 191−256.

(26) Vanommeslaeghe, K.; Hatcher, E.; Acharya, C.; Kundu, S.; Zhong, S.; Shim, J.; Darian, E.; Guvench, O.; Lopes, P.; Vorobyov, I.; MacKerell, A. D. CHARMM General Force Field (CGenFF): A Force Field for Drug-like Molecules Compatible with the CHARMM All-atom Additive Biological Force Fields. *J. Comput. Chem.* **2010**, *31*, 671−690.

(27) Phillips, J. C.; Braun, R.; Wang, W.; Gumbart, J.; Tajkhorshid, E.; Villa, E.; Chipot, C.; Skeel, R. D.; Kale, L.; Schulten, K. Scalable Molecular Dynamics with NAMD. *J. Comput. Chem.* **2005**, *26*, 1781−1802.

(28) Campbell, C. T.; Sellers, J. R. V. The Entropies of Adsorbed Molecules. *J. Am. Chem. Soc.* **2012**, *134*, 18109−18115.

(29) Savara, A.; Schmidt, C. M.; Geiger, F. M.; Weitz, E. Adsorption Entropies and Their Implications for Surface Science. *J. Phys. Chem. C* **2007**, *111*, 8260−8267.

(30) Chai, J.-D.; Head-Gordon, M. Long-Range Corrected Hybrid Density Functionals with Damped Atom-Atom Dispersion Corrections. *Phys. Chem. Chem. Phys.* **2008**, *10*, 6615−20.

(31) Boys, S. F.; Bernardi, F. The Calculation of Small Molecular Interactions by the Differences of Separate Total Energies. Some Procedures with Reduced Errors. *Mol. Phys.* **1970**, *19*, 553−566.

DOI: 10.1021/acs.jpca.6b12653
J. Phys. Chem. A 2017, 121, 3239−3246

(32) Simon, S.; Duran, M.; Dannenberg, J. J. How Does Basis Set Superposition Error Change the Potential Surfaces for Hydrogen-Bonded Dimers? *J. Chem. Phys.* **1996**, *105*, 11024−11031.
(33) Achtyl, J. L.; Vlassiouk, I. V.; Dai, S.; Geiger, F. Interactions of Organic Solvents at Graphene/A-Al2o3 and Graphene Oxide/A-Al2o3 Interfaces Studied by Sum Frequency Generation. *J. Phys. Chem. C* **2014**, *118*, 17745−17755.
(34) Buchbinder, A. M.; Weitz, E.; Geiger, F. M. When the Solute Becomes the Solvent: Orientation, Ordering, and Structure of Binary Mixtures of 1-Hexanol and Cyclohexane over the (0001) A-Al2o3 Surface. *J. Am. Chem. Soc.* **2010**, *132*, 14661−14668.
(35) Redlich, O.; Peterson, D. L. A Useful Adsorption Isotherm. *J. Phys. Chem.* **1959**, *63*, 1024−1024.
(36) Vasanth Kumar, K.; de Castro, M. M.; Martinez-Escandell, M.; Molina-Sabio, M.; Silvestre-Albero, J.; Rodriguez-Reinoso, F. A Continuous Site Energy Distribution Function from Redlich−Peterson Isotherm for Adsorption on Heterogeneous Surfaces. *Chem. Phys. Lett.* **2010**, *492*, 187−192.
(37) Nastaj, J.; Wilczynska, B. Study on Adsorption of Volatile Organic Compounds from Gas Phase on Selected Zeolites. Literature and Experimental Studies on the Adsorption Equilibrium. *Przem. Chem.* **2008**, *87*, 371−376.
(38) Nastaj, J.; Chybowska, M. Adsorption Equilibria of Butan-1-Ol, Toluene and Water Vapour onto Sorbonorit 4 Activated Carbon and the Co-Adsorption of Organic Compounds and Water Vapour onto Skt Activated Carbon. *Adsorpt. Sci. Technol.* **2006**, *24*, 283−300.
(39) Buchbinder, A. M.; Gibbs-Davis, J. M.; Stokes, G. Y.; Peterson, M. D.; Weitz, E.; Geiger, F. M. Method for Evaluating Vibrational Mode Assignments in Surface-Bound Cyclic Hydrocarbons Using Sum-Frequency Generation. *J. Phys. Chem. C* **2011**, *115*, 18284−18294.
(40) Moad, A. J.; Simpson, G. J. A Unified Treatment of Selection Rules and Symmetry Relations for Sum-Frequency and Second Harmonic Spectroscopies. *J. Phys. Chem. B* **2004**, *108*, 3548−3562.
(41) Ishihara, T.; Ishiyama, T.; Morita, A. Surface Structure of Methanol/Water Solutions Via Sum Frequency Orientational Analysis and Molecular Dynamics Simulation. *J. Phys. Chem. C* **2015**, *119*, 9879−9889.
(42) Li, X.; Deng, G. H.; Feng, R. J.; Lin, K.; Zhang, Z.; Bai, Y.; Lu, Z.; Guo, Y. Salt Effect on Molecular Orientation at Air/Liquid Methanol Interface. *Chin. Chem. Lett.* **2016**, *27*, 535−539.
(43) SenGupta, S.; Saha, A.; Kumar, A.; Naik, P. D. Vibrational Sum-Frequency Generation Study of Morpholine at Air-Liquid and Air-Solution Interfaces. *J. Phys. Chem. C* **2016**, *120*, 20132−20141.
(44) Liu, A. A.; Huang, Z.; Deng, G. H.; Guo, Y. Adsorption of Benzonitrile at the Air/Water Interface Studied by Sum Frequency Generation Spectroscopy. *Chin. Sci. Bull.* **2013**, *58*, 1529−1535.
(45) Chen, X. Y.; Boughton, A. P.; Tesmer, J. J. G.; Chen, Z. In Situ Investigation of Heterotrimeric G Protein Beta Gamma Subunit Binding and Orientation on Membrane Bilayers. *J. Am. Chem. Soc.* **2007**, *129*, 12658.
(46) Upshur, M. A.; Chase, H. M.; Strick, B. F.; Ebben, C. J.; Fu, L.; Wang, H.-f.; Thomson, R. J.; Geiger, F. M. Vibrational Mode Assignment of α-Pinene by Isotope Editing: One Down, Seventy-One to Go. *J. Phys. Chem. A* **2016**, *120*, 2684−90.
(47) Strick, B. F.; Delferro, M.; Geiger, F. M.; Thomson, R. J. Investigations into Apopinene as a Biorenewable Monomer for Ring-Opening Metathesis Polymerization. *ACS Sustainable Chem. Eng.* **2015**, *3*, 1278−1281.

DOI: 10.1021/acs.jpca.6b12653
J. Phys. Chem. A 2017, 121, 3239−3246